Published in final edited form as:
Nano Lett. 2009 December ; 9(12): 4049–4052. doi:10.1021/nl9022176.

Self-assembly of lithographically patterned nanoparticles

Jeong-Hyun Cho[1] and **David H. Gracias**[1,2]

[1]Department of Chemical and Biomolecular Engineering, Johns Hopkins University, Baltimore, MD 21218, USA.

[2]Department of Chemistry, Johns Hopkins University, Baltimore, MD 21218, USA.

Abstract

The construction of three dimensional (3D) objects, with any desired surface patterns, is both critical to and easily achieved in macroscale, science and engineering. However, on the nanoscale, 3D fabrication is limited to particles with only very limited surface patterning. Here, we demonstrate a self-assembly strategy that harnesses the strengths of well established 2D nanoscale patterning techniques and additionally enables the construction of stable 3D polyhedral nanoparticles. As a proof of the concept, we self-assembled cubic particles with sizes as small as 100 nm and with specific and lithographically defined surface patterns.

Particles such as nanowires and nanopolyhedra are widely utilized in nanoscale science and engineering, but can be constructed with only limited surface patterning.[1–4] Surface patterning can dramatically alter both the physical and chemical properties of an object.[5–9] There is also a pressing need for strategies to fabricate nanoparticles with any desired surface pattern to enable the bottom-up assembly[10] of artificial crystals and arrays. Here, specific patterns on the surfaces of these particles can direct the assembly via steric forces, lock-and-key interactions and chemical recognition. The inability to construct nanoparticles with any desired surface pattern arises from the fact that although nanoscale patterning techniques such as electron beam lithography (EBL),[11] imprint lithography[12] and scanning probe lithography[13] are extremely precise, they can only be implemented in an inherently two dimensional (2D) manner.

Self-assembly or the spontaneous assembly of interacting precursors to form well ordered particles offers one possible solution to overcome this challenge. Biological self-assembly, for example, enables the construction of extremely complex three dimensionally patterned nanoparticles, such as viruses. In biological assembly, several paradigms such as steric constraints, hierarchical forces and lock-and-key interactions are utilized to direct the assembly by biasing specific outcomes. While some of these paradigms have been explored in meso and microscale fabrication,[10, 14–17] their potential for overcoming the significant challenge of three dimensional nanoscale fabrication has yet to be realized. To enable self-assembly of polyhedral nanoparticles, one could envision utilizing lithography to precisely pattern 2D nanoscale panels with binding sites on their edges; these components can be constructed easily. During assembly, however, when these nanoscale panels are allowed to interact without any additional constraints, a well defined polyhedral particle is highly unlikely to form due to the large number of possible outcomes (Figure 1a). On the other hand, one could bias the desired outcome by joining the nanoscale panels in 2D prior to assembly (Figure 1b). If these panels could then be spontaneously oriented with any desired angle, and subsequently fused to each other, one could

Correspondence and requests for materials should be addressed to D.H.G. (dgracias@jhu.edu).

Supporting Information Available

Details of the fabrication process and figure showing EDS results. The materials is available free of charge via the Internet at http://pubs.acs.org.

in principle construct any nanoscale polyhedral particle with precisely patterned faces. After being precisely assembled on substrates, the polyhedral nanoparticles could subsequently be released by etching or dissolution of the substrate. We provide proof of concept of this strategy by demonstrating the self-assembly of lithographically patterned cubic nanoparticles.

We first fabricated 2D nets with five or six square nanoscale panels and rectangular hinges on silicon (Si) wafer substrates (Figure 1b). The square panels with any desired linear or curved pattern were defined using EBL and lift-off metallization. A second EBL step was used to pattern the hinges. These hinges were precisely aligned between adjacent panels (Figure 1b). The panel dimensions ranged from 100–500 nm in width and 13–29 nm in thickness. The gap between panels was 10–50 nm (10% of the panel dimension). Hinges had lengths of 80–300 nm, widths of 48–450 nm and thicknesses of 26–47 nm. We utilized nickel (Ni) to pattern the panels and tin (Sn) to pattern the hinges of all particles. After patterning arrays of these 2D nets, the wafers were introduced into a planar etcher with oxygen (O_2) and carbon tetrafluoride (CF_4) gases. The five and six-faced particles assembled in the etcher as the hinges reflowed due to heating while the underlying Si substrate was being etched away. The etching of the underlying Si also released the outer panels of the 2D net from the substrate, thereby allowing the particles to self-assemble while still being attached to the substrate through the central panel. The torque needed to orient the panels was generated by the force that results from the minimization of surface energy of the reflowed hinge (Figure 1c). After assembly, polyhedral nanoparticles were released by prolonged etching. The detailed fabrication process is shown in Supporting Information.

Self-assembly based on the minimization of surface energy is an attractive strategy to assemble nanoparticles since these surface forces scale linearly with distance as compared to gravitational forces that scale volumetrically. Therefore, it can be readily seen that at the nanoscale, these surface forces are orders of magnitude larger than gravitational forces. In nanoscale self-assembly, however, several challenges arise. The obvious challenge of patterning the nets with critical dimensions as small as 10 nm was overcome using EBL. When hinges with these small dimensions are defined, factors such as grain size, wetting and reflow significantly affect the patterning and assembly process. To assess optimum grain size and wetting, we experimented with a wide range of evaporation parameters and hinge/panel materials such as copper, gold, silver, zinc, Sn and Ni. The Sn/Ni system worked the best since Sn has intermediate wetting on Ni and Si; thus, the reflowed hinge did not have a strong tendency to spread out of the hinge region and onto the Ni or Si surface. Although we could still observe individual Sn grains at these small size scales, grain coalescence and reflow was observed. Reflow, which refers to liquefaction of the metal, was challenging to achieve since many metals have high melting points and also tend to oxidize. Moreover, the panels needed to be released from the substrate simultaneously during reflow in order to allow them to orient and assemble into the desired 3D particle. Both steps were achieved in approximately 1–2 minutes via a newly discovered reflow process which utilizes a plasma etcher. We experimented with a number of gases such as air, argon (Ar), CF_4, and O_2. We observed, remarkably, that Sn reflowed when exposed to CF_4 / O_2 plasma, but did not reflow when exposed to pure O_2, air, or Ar plasma (Figure 2). We did not observe reflow in the absence of CF_4 / O_2 even when the physical etch parameters such as flow rate, time and power were varied.

Energy dispersive spectroscopy (EDS) characterization (Supporting Information Figure S1) of 50 nm thick Sn films deposited on patterned 10 micron and 200 nm thick square patterns of Ni on Si substrates, before and after etching with the CF_4/O_2 plasma showed the incorporation of approximately 12% atomic concentration of fluorine (F) after etching. We also measured a significant rise in the temperature (over 100 °C) of these thin films deposited on Si substrates during etching with CF_4/O_2. In contrast, a minimal rise in temperature was observed with the Ar plasma on Sn / Si substrates (~10 °C) or with the CF_4 / O_2 plasma on Sn / Al_2O_3 coated Si

substrates (~30 °C). Hence, we conclude that the reaction of the reactive gaseous, fluoride species, primarily with Si (but also to some extent with Sn) during plasma etching generates heat which causes the Sn hinges to reflow. A rise in temperature during the CF_4 / O_2 plasma etching of Si has been documented in prior literature.[18].

We also observed that the angular orientation between panels could be controlled by altering the flow rate of O_2 gas during etching. We investigated this dependence of angular orientation on the assembly of 500 nm nets (Figure 3). On the 500 nm cubic particles, the central panel was unpatterned, while the other four panels had the letters *JHU* patterned on them (Figure 3b and c). In these experiments the flow rate of CF_4 was kept constant at 12 sccm. At low O_2 flow rates of approximately 0.2 sccm, we observed some grain coalescence (of grains less than 50 nm in size) but no significant reflow of large grains (Figure 3d). At these flow rates, approximately 45° angles were observed (Figure 3e and f). A higher O_2 flow rate of approximately 3.6 sccm resulted in grain coalescence, reflow of large grains (Figure 3g) and 90° angles (Figure 3h and i). We rationalize this observation by noting that the observed amount of O_2 concentration needs to be added to CF_4 to increase the concentration of reactive fluorine atoms;[19] these reactive fluorine atoms are essential for both etching and reflow, and hence self-assembly. After the self-assembly process, the particles could be released from the substrate by prolonged etching and they were stable; no obvious change in shape was observed on heating them to 500 °C in air at 1 atm. This feature is critical to the utility of these particles in real world applications and should be contrasted with recent molecular self-assembling paradigms[20] that generate 3D nanopolyhedra which would fall apart when placed in many non-aqueous solvents, in vacuum or on heating. The 500 nm cubic particles were also patterned with curvilinear features having line widths as small as 15 nm (Figure 3i). Additionally, the assembly process could be used with patterned, multilayer panels composed of dissimilar materials. Self-assembly of panels with curvilinear patterns of gold (Au) on Ni resulted in cubic nanoparticles with Au patterns (the letters *J* and *U* with 50 nm line widths) incorporated on the outer faces (Figure 4).

Figure 5 shows EBL patterned 2D nets and resulting self-assembled cubic nanoparticles with overall dimensions of 100 nm. The 100 nm cubes had square patterns with a 30 nm length and the thickness of the panels was 13 nm; the hinge gap between panels was approximately 10 nm (Figure 5a). The 100 nm nanoparticles demonstrated (Figure 5) are magnetic, and hollow, with attoliter encapsulation volumes. These particles assembled while being attached to the substrate (Figure 5d) and we could completely release them from the substrate by prolonged etching.

Our self-assembly process is versatile; it is possible to construct both free standing nanoparticles as well as those attached to substrates. Additionally these particles can be constructed with any desired nanoscale pattern that can be implemented with EBL. In addition to cubic nanoparticles, since the orientation angle between panels can be controlled, this method, in principle, can be used to construct other polyhedral shaped particles. The particles are very stable, and our demonstration of multilayer patterning with dissimilar materials suggests a versatile strategy for the construction of practically applicable patterned, heterogeneous nanoparticles with different combinations of metals, semiconductors and insulators. Since the particles are patterned, we anticipate that they will display novel optical properties, such as unique plasmon resonances. These hollow particles can be used as nanoscale encapsulants; additionally specific surface patterning of Au will enable well defined subsequent molecular patterning using self-assembled monolayers for targeted therapeutics. The particles also represent attractive building blocks for hierarchical self-assembly of nanostructured three dimensional devices.

Supplementary Material

Refer to Web version on PubMed Central for supplementary material.

Acknowledgments

This research was supported by the NIH Director's New Innovator Award Program, part of the NIH Roadmap for Medical Research, Grant No. 1-DP2-OD004346-01 and by the National Science Foundation (NSF) Grant No. 0854881.

References

1. Qin L, Park S, Huang L, Mirkin C. Science 2005;309:113. [PubMed: 15994551]
2. Zhang Z, Glotzer SC. Nano Lett 2004;4:1407.
3. Jackson AM, Myerson JW, Stellacci F. Nat. Mater 2004;3:330. [PubMed: 15098025]
4. Srinivas G, Pitera JW. Nano Lett 2008;8:611. [PubMed: 18189443]
5. Gleiche M, Chi LF, Fuchs H. Nature 2000;403:173. [PubMed: 10646597]
6. Curtis ASG, Casey B, Gallagher JO, Pasqui D, Wood MA, Wilkinson CD. Biophys. Chem 2001;94:275. [PubMed: 11804737]
7. Turner S, Kam L, Isaacson M, Craighead HG, Shain W, Turner J. J. Vac. Sci. Technol. B 1997;15:2848.
8. Rastegar A, Skarabot M, Blij B, Rasing T. J. Appl. Phys 2001;89:960.
9. Gay G, Alloschery O, Viaris de Lesegno B, O'Dwyer C, Weiner J, Lezec HJ. Nat. Phys 2006;2:262.
10. Grzybowski B, Whitesides GM. Science 2002;295:2418. [PubMed: 11923529]
11. Beaumont SP, Bower PG, Tamamura T, Wilkinson CDW. Appl. Phys. Lett 1981;38:436.
12. Chou SY, Krauss PR, Renstrom PJ. Science 1996;272:85.
13. Liu G-Y, Xu S, Qian Y. Acc. Chem. Res 2000;33:457. [PubMed: 10913234]
14. Terfort A, Bowden N, Whitesides GM. Nature 1997;386:162.
15. Gracias DH, Tien J, Breen TL, Hsu C, Whitesides GM. Science 2000;289:1170. [PubMed: 10947979]
16. Syms RRA, Yeatman EM, Bright VM, Whitesides GM. J. Microelectromech. Syst 2003;12:387.
17. Leong TG, Lester PA, Koh TL, Call EK, Gracias DH. Langmuir 2007;23:8747. [PubMed: 17608507]
18. Magunov AN. Instrum. Exp. Techniques 2000;43:133.
19. Mogab CJ, Adams AC, Flamm DL. J. Appl. Phys 1978;49:3796.
20. He Y, Ye T, Su M, Zhang C, Ribbe AE, Jiang W, Mao C. Nature 2008;452:198. [PubMed: 18337818]

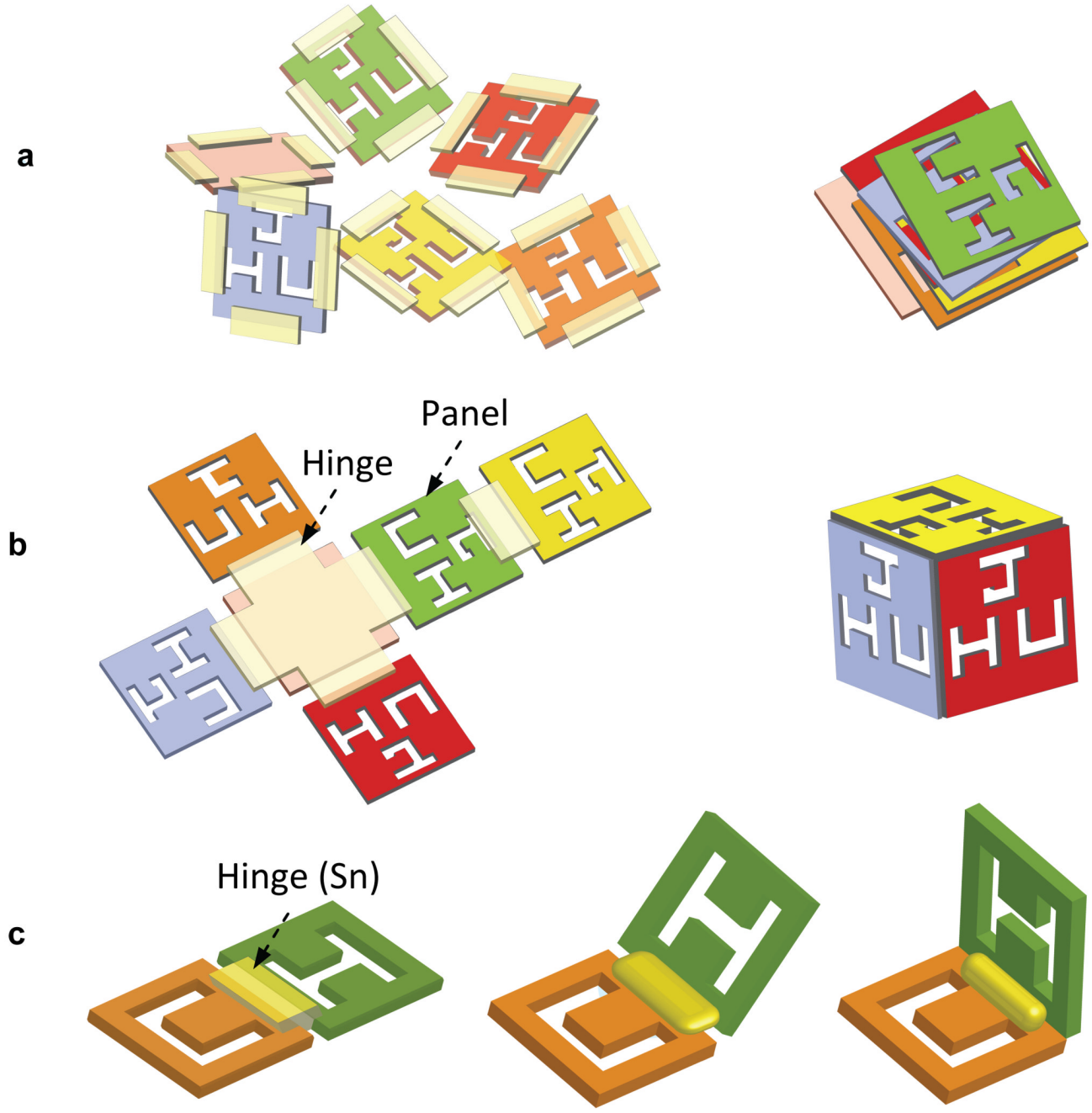

Figure 1.
Schematic diagram showing the concept behind the self-assembly process. (a) Patterned panels with binding sites that interact without constraints are unlikely to self-assemble into cubes. (b) Joining panels to form nets limits the possible interactions and allows them to assemble correctly to form a nanocube. (c) Self-assembly is driven by the reflow of tin (Sn) within the hinges of the net; the panel angular orientation needed for self-assembly is derived from the force that is generated when the reflowed hinges minimize their surface area.

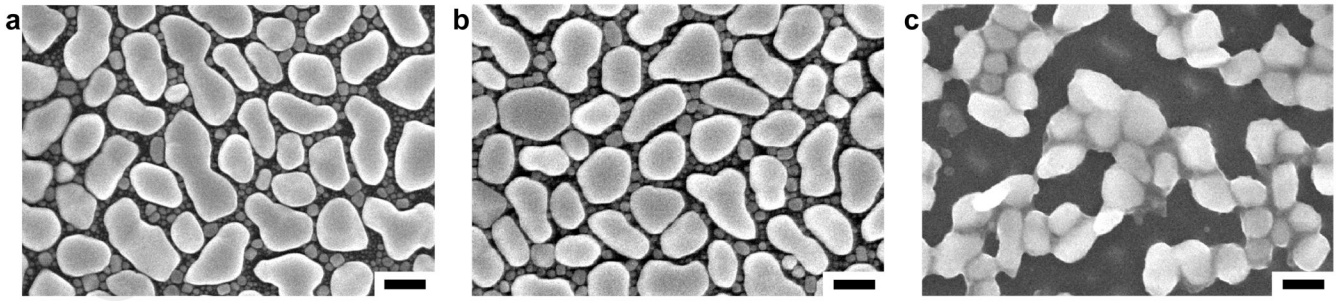

Figure 2.

Scanning electron microscopy (SEM) images showing results of experiments investigating Sn reflow in a plasma etcher. (a) A 50 nm thick Sn film evaporated on a silicon wafer prior to reflow. (b) The Sn film after exposure to an Ar plasma with a 10 sccm flow rate for 2 minutes; no reflow or significant change was observed. (c) The Sn film after exposure to a O_2/CF_4 plasma with a 3.6 and 12 sccm flow rate of O_2 and CF_4 respectively for 2 minutes_; significant reflow was observed. Scale bars: 200 nm.

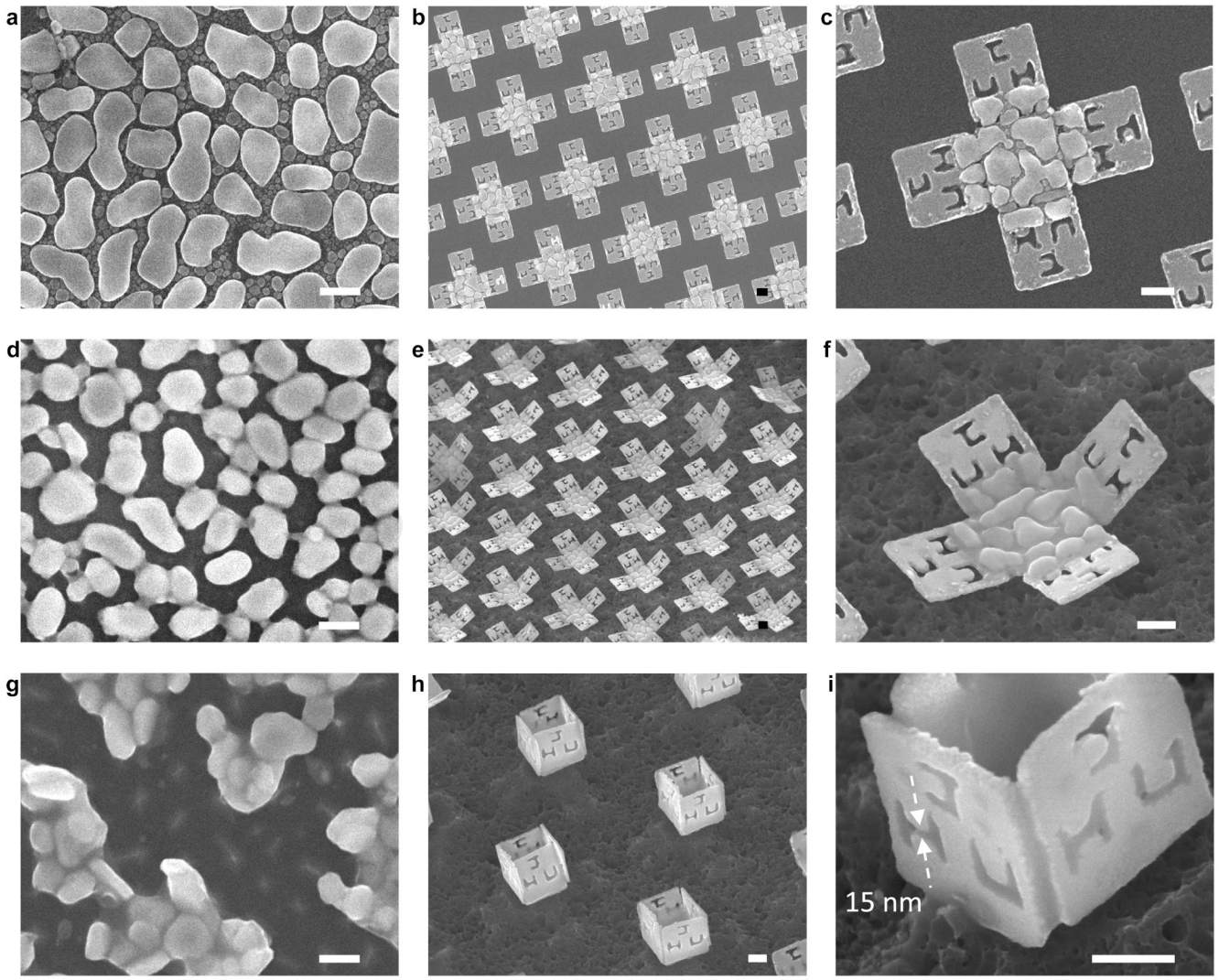

Figure 3.

Results of experiments demonstrating that the orientation angle can be controlled by varying the ratio of O_2 to CF_4. SEM images of Sn thin films on a silicon wafer and 500 nm sized 2D nets before and after plasma etching. (a–c) Images of a Sn thin film and 2D nets before plasma etching. (a) 50 nm thick Sn on a silicon wafer. (b), (c) Progressively zoomed-in images of Ni panels with Sn hinges. (d–f) Images of the Sn film and 2D nets after plasma etching with a 0.2 and 12 sccm flow rate of O_2 and CF_4 respectively. (d) The Sn film shows some grain coalescence (of grains less than 50 nm in size) but no significant reflow of large grains. (e),(f) Progressively zoomed-in images showing that the 2D nets assemble with angles of approximately 45° under these conditions. (g–i) SEM images of the Sn film and 2D nets after plasma etching with a 3.6 and 12 sccm flow rate of O_2 and CF_4 respectively. (g) The Sn film shows considerable reflow. (h) Progressively zoomed-in images showing that the 2D nets assemble with angles of approximately 90° under these conditions. It should be noted that the assembly process is parallel and (i) the particles have the letters *JHU* patterned with line widths as small as 15 nm. Scale bars: 200 nm.

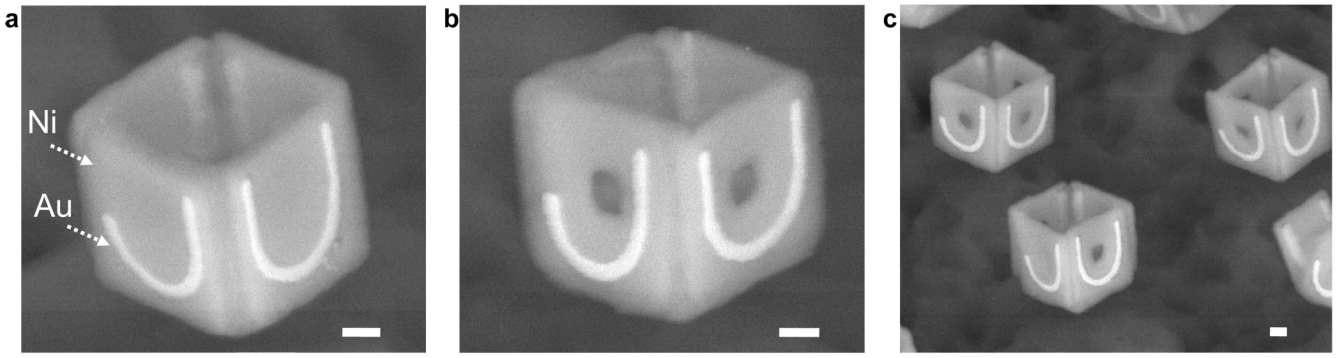

Figure 4.
SEM images of 500 nm scale cubic particles patterned with dissimilar materials. The particles have 20 nm thick curvilinear patterns of Au defined precisely with the letters *J* and *U* with 50 nm line widths on the outer faces of Ni. The SEM images were captured using a back scatter detector which is sensitive to the atomic mass; hence the Au appears brighter than Ni. (a) SEM image of a patterned cubic particle of Au on Ni. (b) In addition to the pattern of Au on Ni, the particle also has 100 nm square holes within each face. (c) SEM image showing the parallel nature of the assembly with yields of approximately 30 %. Scale bars: 100 nm.

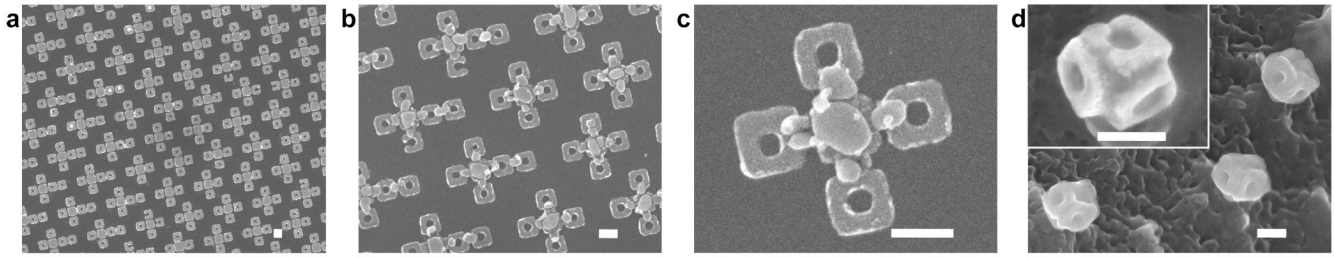

Figure 5.
SEM images of 100 nm scale cubic particles before and after self-assembly. (a) Lithographically patterned Ni panels whose surfaces were patterned with 30 nm squares. (b) Lithographically patterned Sn hinges on Ni panels. (c) A magnified image of the hinges and panels. (d) 100 nm scale cubic particles after self-assembly. Scale bars: 100 nm.